

SPIRAL SECTOR MAGNET OF RCNP RING CYCLOTRON PROJECT

K. Hosono, I. Miura, M. Kibayashi, M. Inoue and A. Shimizu
 Research Center for Nuclear Physics, Osaka University,
 Ibaraki 10-1, Osaka 567, Japan

ABSTRACT

An intermediate energy particle accelerator system has been designed as a new facility at RCNP. A 1/4.5-scale model magnet of spiral sector have been made to study various field properties and orbit properties. Some results on the model magnet are presented.

INTRODUCTION

An intermediate energy particle accelerator complex which can accelerate protons up to 300 MeV has been designed as a new facility at RCNP¹. This accelerator complex consists of a separated sector cyclotron (ring cyclotron) and an injector cyclotron. The characteristics of this system are given in Table 1. The ring has four spiral sectors and the sector magnets have 6 cm gap.

A 1/4.5-scale model magnet has been made to study various magnetic field properties². Magnetic field measurements have been made using eight Hall generators that are positioned by a high precision numerically controlled apparatus³. The magnetic field characteristics of the model and the results of orbital analyses using the measured fields are described in this report.

MODEL MAGNET AND FIELD MEASUREMENT

A 1/4.5-scale model of the spiral sector magnet² of the ring, weighing about 5 tons, has been made and is shown in Figs. 1 and 2. The pole pieces are made of low carbon forged iron. The radial pole edges are shaped stepwise into a Rogowski's curve with a numerically controlled milling machine. The yoke is divided into three pieces. Each piece of yoke is low carbon casted iron degassed before casting.

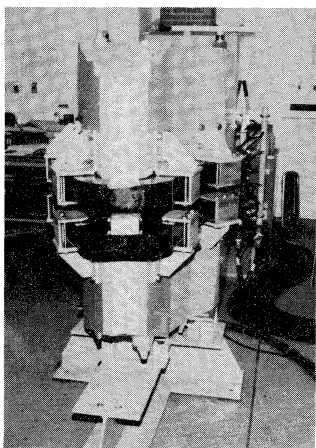


Fig. 1. Photograph of the 1/4.5-scale model magnet of the ring.

Table 1

Design parameters of the spiral sector magnet of the ring cyclotron with the parameters of the injector.

	Injector Cyclotron	Ring
	AVF	SPIRAL SECTOR
No. of sector magnets	4	4
Sector angle		34~39°
Injection radius (cm)		136
Extraction radius (cm)	68	375
Magnet gap (cm)	13.0	6.0
Max. magnetic field (kG)	20.0	15.5
Proton max. energy (MeV)		300
Alpha particle energy (MeV)		320
K-value	70	280
Weight of magnet (ton)	120	1600
Main coil magnet (kW)	200	350
No. of trim coils	8	35
Trim coil power (kW)	20	170
No. of cavities	2	2
RF frequency (MHz)	20~33	20~33

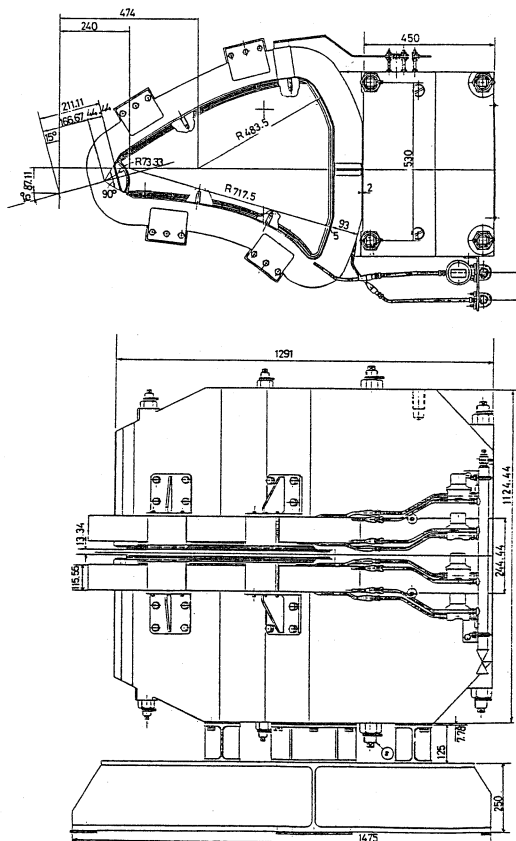


Fig. 2. Plan and side views of the 1/4.5-scale model magnet of the ring.

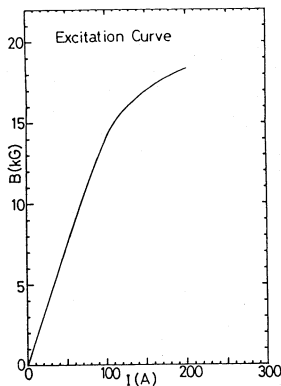


Fig. 3. Measured excitation curve of the model magnet of spiral sector.

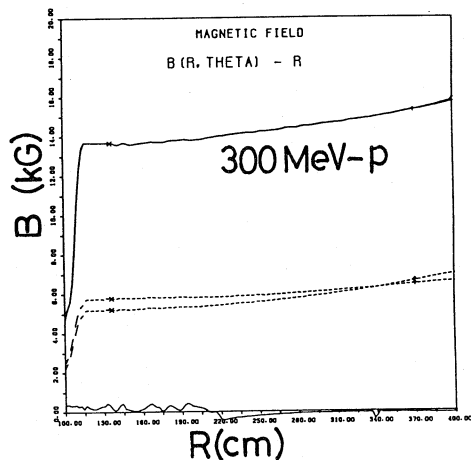


Fig. 4. An example of the measured field maps.

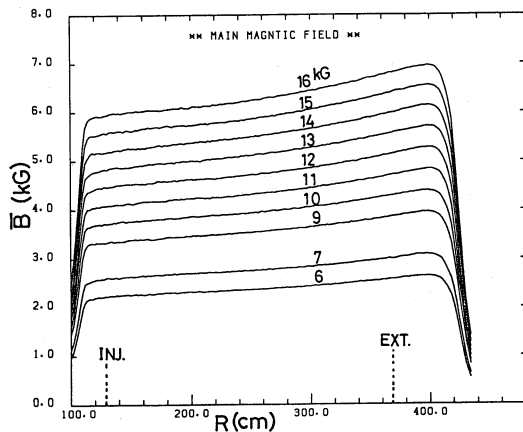


Fig. 5. Strength of the average magnetic fields as a function of full-scale radius.

Magnetic field mapping has been made on a cartesian grid. Eight Hall generators were used for the magnetic field measurements. The Hall generators were mounted on an aluminum arm stretched from a probe carriage. The magnetic field mapping, the data acquisition, reduction and storage were automatically controlled by a PDP-11/10 computer and CAMAC system.

The magnetic field profiles of the model were mapped at excitation levels of 5-16 kG. The excitation curve is shown in Fig. 3. An example of the measured field maps is shown in Fig. 4. We corrected the values of the field in the valley region using the simple superposition of $B(R, \theta) = B(R, \theta) +$

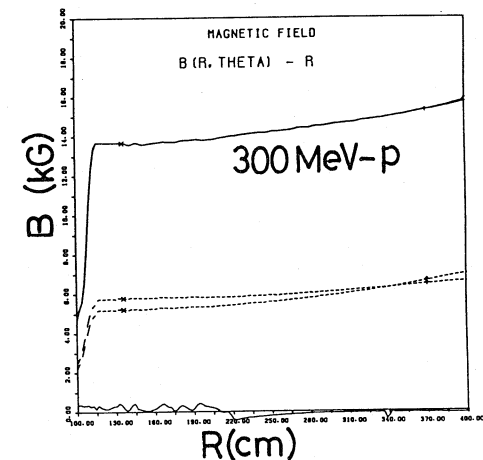


Fig. 6. Orbital-shape isochronous field and the radial and vertical frequencies for 300 MeV protons calculated using a measured field.

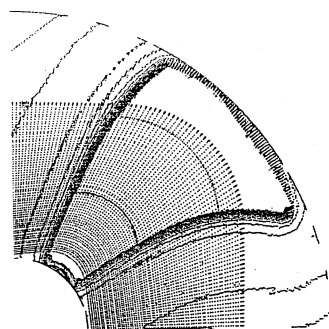


Fig. 7. Equilibrium orbits calculated using a measured field.

$B(R, \theta + \pi/2)$ ($0 \leq \theta \leq \pi/4$) or $B(R, \theta) = B(R, \theta) + B(R, \theta - \pi/2)$ ($\pi/4 < \theta \leq \pi/2$), on considering effects of a neighbouring magnet. Fig. 5 shows the strength of average magnetic fields as a function of full-scale radius for various excitation levels. There is little difference in field shape in the range between the injection (136 cm) and the extraction (375 cm) radii. Little absence of saturation effects leads to nearly the same dynamics of particle orbits at low and high field levels.

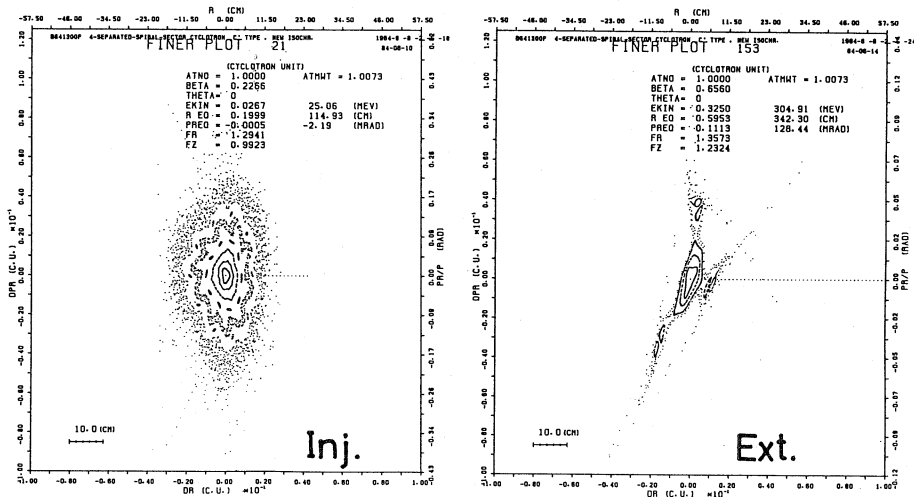


Fig. 8. Phase plots at the injection and the extraction radii for 300 MeV protons calculated using a measured field.

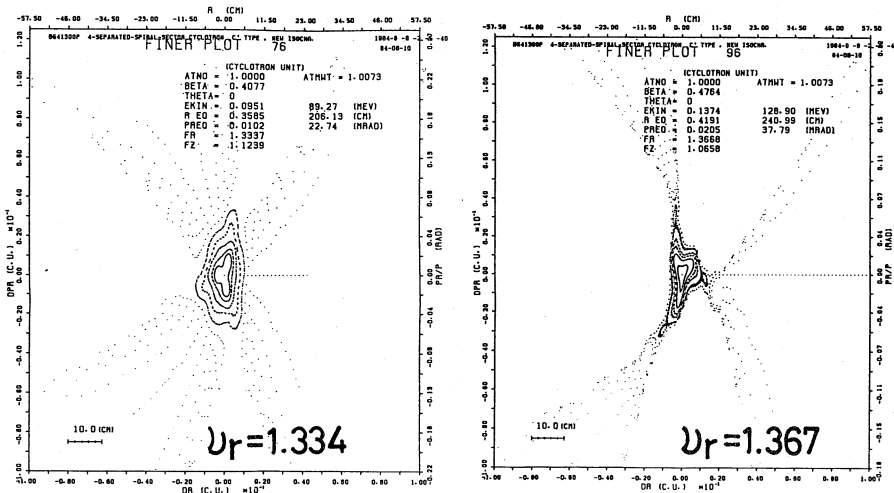


Fig. 9. Phase plots near $\nu_r = 4/3$ resonance calculated using a measured field.

ORBIT PROPERTIES

Orbit properties of the ring with four spiral sectors have been studied using the measured magnetic fields. Fig. 6 shows the calculated orbital-shape isochronous field and radial and vertical frequencies for 300 MeV of protons. Fig. 7 shows the equilibrium orbits. Fig. 8 shows the phase plots of 300 MeV protons at the injection and the extraction radii. We can obtain wide stable region as shown in fig. 8. The problem encountered in the four spiral sector ring cyclotron is the $\nu_r = 4/3$ resonance. It is important to examine the effect of $\nu_r = 4/3$ resonance for beam stability. Fig. 9 shows the phase plots near the $\nu_r = 4/3$ resonance. We have calculated the accelerating orbits and studied beam stability near the $\nu_r = 4/3$ resonance. We have concluded that the effect of the $\nu_r = 4/3$ resonance is not so serious in acceleration by the four spiral sector cyclotron.

From the results of the measured fields and calculations, we concluded that the requirements for the spiral sector magnets of

the ring cyclotron were fulfilled sufficiently. As a further aid to design, we are making a model of trimming coils, in order to produce the required radial field gradient, and to determine the positions and widths of the trimming coils.

REFERENCES

1. I. Miura et al., RCNP Annual Report (1983) p.145.
2. K. Hosono et al., RCNP Annual Report (1983) p.151.
3. K. Hosono et al., Proc. 9th Int. Conf. on Cyclotron and Their Applications, Caen (1981) p.379.